



Effect of green tea-loaded chitosan nanoparticles on leathery dentin microhardness

Fabiana Almeida Curylofo-Zotti¹ · Antonio Claudio Tedesco² · Gustavo Teodoro Costa Lizarelli¹ · Luandra Aparecida Unten Takahashi² · Silmara Aparecida Milori Corona¹

Received: 3 December 2020 / Accepted: 28 April 2021 / Published online: 8 May 2021
© The Society of The Nippon Dental University 2021

Abstract

The purpose of this study was to assess the effect of a chitosan-based nanoformulation containing green tea on leathery (remaining) dentin subsurface microhardness. Size distribution, polydispersity index (PDI) and zeta potential (mV) of nanoformulations were previously determined by dynamic light scattering (DLS). Human dentin specimens were exposed to *Streptococcus mutans* for 14 d. Soft dentin were selectively removed by Er:YAG laser ($n = 30$) or bur ($n = 30$). Remaining dentin was biomodified with chitosan nanoparticles (Nchi, $n = 10$) or green tea-loaded chitosan nanoparticles (Gt + Nchi, $n = 10$) for 1 min. Control group ($n = 10$) did not receive any treatment. Subsurface microhardness (Knoop) was evaluated in hard (sound) and soft dentin, and then, in leathery dentin and after its biomodification, at depths of 30, 60 and 90 μm from the surface. Nchi reached an average size of ≤ 300 nm, PDI varied between 0.311 and 0.422, and zeta potential around +30 mV. Gt + Nchi reached an average size of ≤ 350 nm, PDI < 0.45 , and zeta potential around +40 mV. Soft dentin showed significantly reduced microhardness at all depths ($p > 0.05$). The subsurface microhardness was independent of choice of excavation method ($p > 0.05$). At 30 μm from the surface, Gt + Nchi increased the leathery dentin microhardness compared to untreated group ($p < 0.05$). Nchi promoted intermediate values ($p > 0.05$). Both nanoformulations showed an average size less than 350 nm with nanoparticles of different sizes and stability along the 90-day period evaluated. Subsurface microhardness of bur-treated and laser-irradiated dentin was similar. At 30 μm , the biomodification with Gt + Nchi improved the microhardness of leathery dentin, independently of caries excavation method used.

Keywords Nanoparticles · Er:YAG laser · Bur · Caries-affected dentin

Introduction

A complex biological substrate involving different patterns of dentin may be found during caries excavation. In shallow or moderately deep cavitated dentin lesions (radiographically extending less than the pulpal third or quarter of dentin), the selective removal to firm dentin is recommended for both the primary and permanent dentitions [1, 2]. The

selective removal to firm dentin leaves ‘leathery’ dentin over the pulp chamber. This dentin consistency is often described as caries-affected dentin, being the ‘leathery’ dentin, a transition on the spectrum between soft and firm dentin [1]. Caries-affected dentin is a demineralized substrate with loss in the crystallinity of the mineral phase [1, 2]. Additionally, the organic components are disorganized with considerable changes in the secondary structure of the collagen matrix [3]. All these modifications in the dentin ultrastructure are expected to decrease its mechanical properties [4].

Different excavation methods have been proposed for carious tissue removal [1]. Er:YAG laser (erbium-doped:yttrium–aluminium-garnet laser) has been studied as a possible substitute for burs during caries excavation [5–9]. Er:YAG laser irradiation causes minimal thermal side effects on surrounding tissue [10]. Less vibration, pressure, and noise during cavity preparation [11, 12] and less need for the local anesthesia have been reported

✉ Fabiana Almeida Curylofo-Zotti
curylofozotti@usp.br

¹ Department of Restorative Dentistry, School of Dentistry of Ribeirão Preto, University of São Paulo, Café Avenue, s/n, Ribeirão Preto, São Paulo 14040-904, Brazil

² Department of Chemistry, Center of Nanotechnology and Tissue Engineering -Photobiology and Photomedicine Research Group, Faculty of Philosophy, Sciences and Letters of Ribeirão Preto, University of São Paulo, São Paulo, Brazil

to be positive aspects of this system [13]. Carious dentin has about 2.7 times more water than sound dentin [14]. Er:YAG laser has a wavelength of 2.94 μm , which is located in the middle of the infrared region of the electromagnetic spectrum. The 2.94- μm wavelength correspond to the same peak absorption range of hydroxyapatite crystals, and to the large absorption band of water. During Er:YAG laser irradiation, the energy absorbed by water molecules of dentin organic content leads to successive micro explosions which causes ejection of organic and inorganic substrate [15].

Chitosan-based nanomaterials have versatile physico-chemical characteristics, considered to be a potential target for biological applications [16]. Chitosan is a natural polymer obtained by alkaline hydrolysis of chitin; consisting of randomly distributed β -(1,4)-linked D-glucosamine (deacetylated) and N-acetyl-D-glucosamine (acetylated units) [17]. Chitosan is biocompatible, non-toxicity, biodegradable [18], and has good antimicrobial activity against various isolated species and biofilms [19–21]. Chitosan nanoparticles may be produced using an aqueous acidic solution, avoiding the use of hazardous organic solvents. The functional groups, hydroxyl ($-\text{OH}$) and amine ($-\text{NH}_2$), present in chitosan allow the reaction with cross-linking agents for in situ chemical cross-linking [22]. Besides that, chitosan nanoparticle shows the ability to control the release of other active agents [23, 24].

Green tea, obtained from less fermented leaves of *Camellia sinensis*, is rich in catechins such as epicatechin (EC), epigallocatechin (EGC) and Epigallocatechin-3-gallate (EGCG) [25, 26]. Green tea polyphenols have been reported to possess various biological properties, including antioxidant, anti-carcinogenic, and anti-inflammatory activities [26]. When chitosan is dissolved in an acid medium, its amino groups may be protonated resulting in a positive charge, which gives rise to its bioadhesive ability to negative charged surfaces, such as the tooth [27]. This could be one of the reasons why chitosan may act as mechanical barrier for acid penetration, for example, in the enamel, inhibiting its demineralization [28]. The formation of surface deposits of organic materials was observed after dentin treatment with green tea, which could be explained by the presence of induced collagen crosslinks [29]. However, green catechin polyphenols can undergo degradation, and may be easily oxidized at relatively high temperature, oxygen concentration and pH [30, 31]. Thus, the nanoencapsulation approach could protect the polyphenols against its degradation; and the target delivery system (TDS) could restore the mechanical properties of remaining dentin. This preliminary study aimed to evaluate the effect of a chitosan-based nanoformulation containing green tea or not on microhardness of the leathery (remaining) dentin after the selective removal by bur and Er:YAG laser.

Materials and methods

Preparation of chitosan nanoformulation (Nchi)

Chitosan nanoparticles were prepared according to ionic cross-linking method using tripolyphosphate (TPP) [22]. Low molecular weight chitosan (#448869, Sigma-Aldrich, Darmstadt, Germany) was dissolved in 0.33% (vol/vol) glacial acetic acid for a stock solution of 2 mg/mL. The pH was adjusted to 5 using 0.1 N sodium hydroxide. Under mild stirring, TPP solution (1 mg/mL) was slowly added, drop by drop, to chitosan solution. The proportion of chitosan to TPP was 5:1.

Extraction of the green tea mass and preparation of green tea chitosan nanoformulation (Gt + Nchi)

Green tea (Green tea extract 400 mg, NOW Supplements, USA) were submitted to ultrasound bath for 10 min and centrifuged at 10,000 rpm for 15 min. The supernatants were pooled. Under constant stirring, supernatants were added, drop by drop continuously and slowly, to chitosan solution. After 30 min of stirring, the TPP was added to solution according to previously described protocol [22]. The final solution of Gt + Nchi contained 0.3% (w/w) of green tea and was kept at $-4\text{ }^\circ\text{C}$ until use.

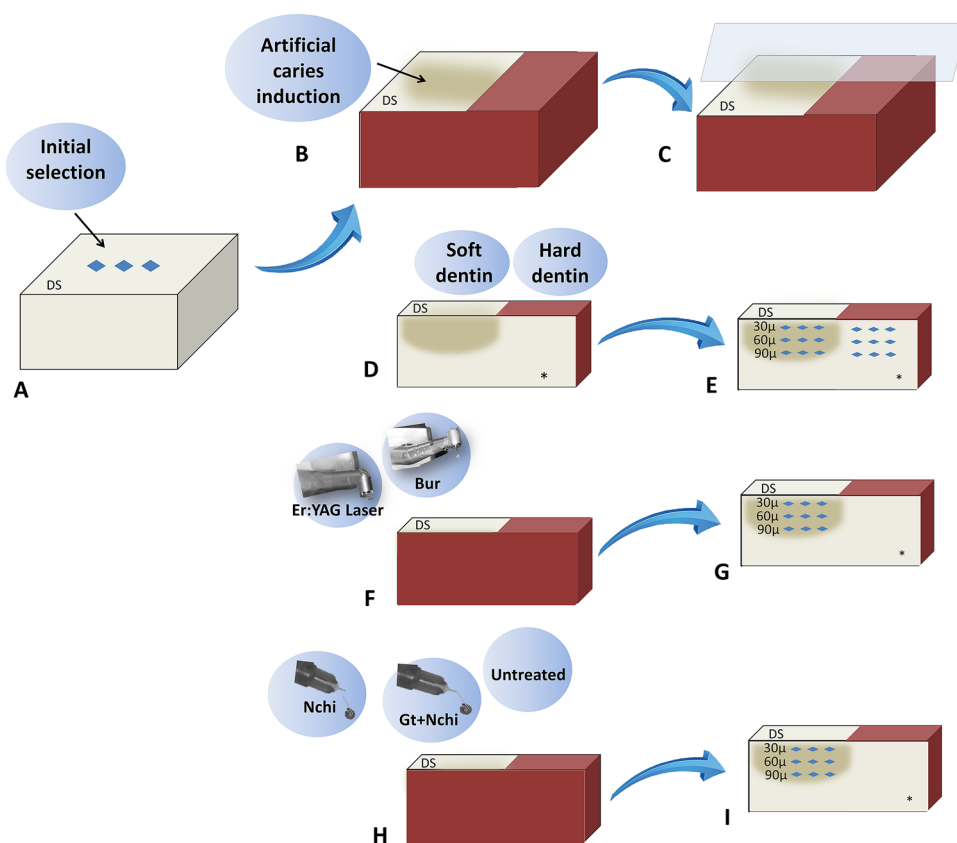
Characterization of chitosan-based nanoformulations (Nchi and Gt + Nchi)

Size distribution, polydispersity index (PDI) and zeta potential of the nanoformulations were determined using a Zetasizer Nano Series (Malvern Instrumentation Co, Westborough, MA). 20 μL of each solution were diluted in 2 mL of milli-Q water using a clear plastic cuvette. The size and polydispersity index were determined using photon correlation spectroscopy at $25\text{ }^\circ\text{C}$ and scattering angle of 173° . Zeta potential was determined using a disposable capillary zeta potential cell (Malvern DTS1060) by means of the electrophoretic mobility of the particles. The DLS measurement for average size, PDI and zeta potential were monitored over a window of time of 90 days after preparation. The Nchi was monitored over a period of 75 days and the Gt + Nchi during a period of 88 days, as presented in Fig. 1.

Tooth selection and specimen preparation

Human third molars were obtained from the Human Biobank Teeth of University of São Paulo (Institutional Review Board protocol CAAE 69600217.4.0000.5419). Teeth were cleaned and analyzed under a stereomicroscope

Fig. 1 Schematic representation of the microhardness evaluations. **a** Initial selection ($n=60$) of dentin specimens based on their microhardness value. **b** Artificial caries induction by *S. mutans*. **c** Cross-section of dentin specimen for evaluation of subsurface. **d** Indentations on hard and soft dentin subsurfaces. **e** Selective removal of carious lesions by Er:YAG laser ($n=30$) or Bur ($n=30$). **f** Indentations on leathery (remaining) dentin. **g** Treatment with Nchi ($n=10$), Gt+Nchi ($n=10$), and untreated group ($n=10$). **h** Indentations on treated dentin



(Leica S6 D Stereo Zoom, Leica Microsystems AG, Switzerland). Teeth with no structural defects were selected. Roots were sectioned in the cementum enamel junction with a double-faced diamond disk mounted in a cutting machine (Isomet 1000, Buehler, Lake Bluff, IL, USA). Specimens had the enamel removed and one specimen with the dimensions of $6.0 \times 6.0 \times 2.5$ mm was obtained from each tooth. Dentin surface was polished up to 1200-grit Al_2O_3 abrasive paper (DP-9U2, Struers A/S, Copenhagen, Denmark). Specimens were immersed in deionized water and sonicated for 10 min to remove polishing residues. At this point, the surface microhardness using a microhardness tester (HMV-2000, Shimadzu Corporation, Kyoto, Japan) was tested. Indentations were taken using a diamond penetrator for Knoop hardness (KHN) with a load cell of 50 g on sound dentin and 25 g on carious dentin, both for 15 s [5]. For each specimen, three measurements were performed with 100 μm spacing between each indentation. The dentin specimen was selected based on the average microhardness value found (52.07 KHN). Specimens with microhardness average 20% below or 20% above of the overall average were discarded. Sixty sound molars ($n=10$) were selected.

Artificial caries induction

To obtain a reference area in dentin to determine the readings in depth, the lateral surfaces and the half occlusal surface of each dentin specimen were painted with two layers of cosmetic varnish (Colorama Maybelline Ltda, Sao Paulo, Brazil). Specimens were sterilized using the following gases mixture: 30% ethylene oxide and 70% carbon dioxide at 50–55 °C for 4 h. Artificial lesions were created according to a previous study [32]. Briefly, specimens were aseptically placed in a beaker containing an artificial caries solution. The solution contained 100 mL of distilled water, 3.7 g of brain heart infusion culture (BHI), 0.5 g of yeast extract, 1.0 g of glucose, 2 g of sucrose and 100 μL of primary culture of *Streptococcus mutans* ATCC25175, pH=4.0. Specimens were incubated at 37 °C in a microaerophilic jar (BBL GasPak system, Becton–Dickinson, Franklin Lakes, EUA), and at every 48 h, specimens were transferred to a fresh solution. At 14 days, the biofilm was carefully removed, and the specimens were washed in distilled water. Then, each specimen was sectioned in half, and the dentin along the long axis of the carious lesion (subsurface) was polished with 1200-grit Al_2O_3 abrasive paper (DP-9U2, Struers A/S,

Copenhagen, Denmark) to remove the risks from the cutting disc. Specimens were immersed in deionized water and sonicated for 10 min to remove polishing residues. Indentations were taken using a diamond penetrator for Knoop hardness (KHN) with a load cell of 25 g for 15 s [5] at three depths: 30, 60 and 90 μm from the dentin surface. For each specimen, three measurements were performed with 100 μm spacing between each indentation in both areas of the specimen (sound and soft dentin).

Selective removal of soft dentin

The selective removal of soft dentin was standardized using an automatic custom-designed device (MPC ElQuip, São Carlos, Sao Paulo, Brazil) as previously reported [6], and only one operator performed these procedures. Briefly, the erbium-doped yttrium aluminium-garnet laser (Er:YAG laser, R02 tip, Fidelis Er III, Fotona, Ljubljana, Slovenia) was applied at noncontact mode with focal distance of 7 mm, pulse energy of 250 mJ, pulse repetition rate of 4 Hz, an output beam diameter of 0.9 mm, energy density of 39 J/cm², and under water spray (6 mL/min). In the control group, soft dentin was performed using a round carbide bur #8 (KG Sorensen, Barueri, SP, Brazil) at low speed (1:1 L micro-series, Bien-Air Dental, CA, USA). The criteria of removal were based on the dentin consistency. The tactile softened dentin was completely removed until the leathery dentin was found. A sharp probe was used to check the dentin consistency, when the sharp probe is pressed onto it, soft dentin deforms with a latent ‘stickiness’. In addition, the softened dentin was easily scooped up with a sharp hand excavator with little force applied. Leathery dentin (remaining) show more resistance against to deformation when an instrument is pressed onto it [1]. After selective removal, indentations were taken using the same protocol previously described.

Treatment with nanoformulations

The dentin specimen was treated with 50- μL Nchi ($n = 10$) or Gt + Nchi ($n = 10$) for 1 min, followed by rinsing with distilled water for 15 s and drying with absorbent paper. Control specimens ($n = 10$) did not receive any treatment. Again, dentin specimens were subjected to microhardness evaluations. Figure 1 shows a schematic representation of all-time points when indentations performed.

Data analysis

The data presented normal distribution. Therefore, data were statistically analyzed by Three-Factors Repeated Measures ANOVA, followed by Tukey’s post hoc test ($\alpha = 0.05$), using SPSS version 20.0 (SPSS Inc., v20, Chicago, IL, USA).

Results

Chitosan nanoparticles reached an average size of less than 300 nm. The polydispersity index varied between 0.311 and 0.422, which indicates nanoparticles of different sizes. The zeta potential is around +30 mV, considered strongly cationic. Chitosan nanoparticles containing green tea reached an average size of less than 350 nm. The polydispersity index is smaller than 0.45, and the zeta potential are around +40 mV. Low variation along the average of 90-day period of evaluation (75 days for Nchi and 88 days for Gt + Nchi) indicate the long-term stability of the nanoformulations (Fig. 2).

Artificial carious lesions induced by *S. mutans* biofilm significantly reduced dentin microhardness at depths of 30, 60 and 90 μm from the surface ($p < 0.05$). The lower microhardness values were found at 30 μm , 60 ($p < 0.05$) and 90 μm ($p < 0.05$), respectively. After selective caries removal, no differences were found between soft and leathery dentin ($p > 0.05$). The subsurface microhardness was independent of choice of excavation method ($p > 0.05$, Table 1).

The interaction between depth vs treatment was significant ($p < 0.05$). At 30 μm from the surface, the treatment with Gt + Nchi increased the microhardness of the leathery dentin when compared to untreated group ($p = 0.032$). The treatment with Nchi promoted intermediate values, not statistically different from untreated and Gt + Nchi groups ($p > 0.05$). The subsurface microhardness of untreated dentin increased accordingly: 30 < 60 < 90 μm ($p < 0.05$). Treatment with Nchi and Gt + Nchi increased the microhardness of the dentin subsurface, and no difference was observed between the different depths ($p > 0.05$, Table 2).

Discussion

Reduction in microhardness values is directly related to dentin mineral loss [33]. Mineral loss was higher in the most superficial zone, at 30 μm from the dentin surface. Clinically, caries excavation has been centered around levels of hardness of the remaining dentin [1], which subjectively can be described as soft, leathery, firm and hard. Histologically, the soft dentin (often described as caries-infected dentin) is composed by a non-remineralizable necrotic collagen matrix with the presence of bacteria. In the leathery dentin (also known as caries-affected dentin), the number of bacteria is reduced, and the collagen fibrils are denatured. However, when the acid exposure is removed, this tissue has an innate ability to remineralize [34, 35].

Two caries removal techniques were investigated in the present study, the carbide bur with a low-speed handpiece

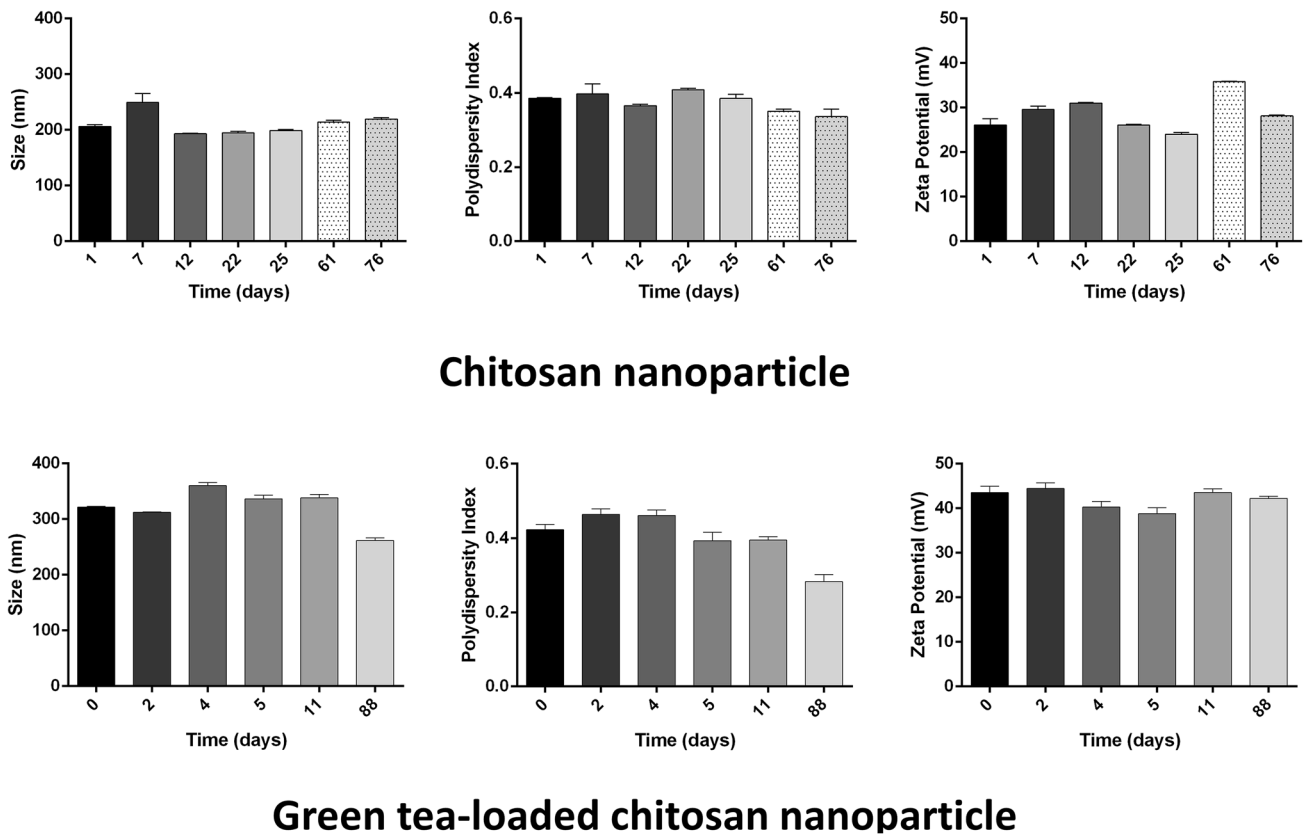


Fig. 2 Characterization of Nchi and Gt+Nchi (Size distribution, Polydispersity index, Zeta potential)

Table 1 Average (standard deviation) of microhardness values (KHN) found according to the depth in the different types of dentin substrate

Dentin substrate / Method of removal	Depth		
	30	60	90
Hard dentin (sound)	37.99 (12.30) ^{A,a}	38.39 (13.35) ^{A,a}	38.29 (13.22) ^{A,a}
Soft dentin	16.90 (5.33) ^{A,b}	22.08 (8.85) ^{B,b}	24.93 (9.76) ^{C,b}
Leathery dentin / Bur	17.39 (5.96) ^{A,b}	25.38 (11.75) ^{B,b}	29.07 (12.92) ^{C,a,b}
Leathery dentin / Er:YAG Laser	19.70 (4.41) ^{A,b}	26.77 (10.57) ^{B,b}	29.00 (11.25) ^{C,b}

Different capital letters indicate a statistically significant difference in the same line

Different lowercase letters indicate a statistically significant difference in the same column

Three-way ANOVA, Tukey's post hoc test ($\alpha=0.05$)

which is considered the conventional method, and the high-intensity Er:YAG laser. Only the soft dentin was removed due to the need of simulate the influence of both methods on leathery (remaining) dentin before treatment with the bio modifiers. Our results showed bur-treated and laser-irradiated dentin had similar behavior, the two tested techniques were similarly efficient to remove softened dentin tissue. Despite the remaining leathery dentin being a substrate frequently found in clinical practice, there is a lack of information about the influence of excavation methods on this type of substrate. The conventional method of caries removal with carbide bur can remove

both soft and sound dentin. However, when used carefully, it is an adequate method for removing only softened tissue. The Er:YAG laser provides an adequate precision during caries removal because of its higher absorption in the humid carious tissue. This allows for conservative caries excavation without extending the preparation into sound tooth structure [36]. The Er:YAG laser irradiation yields a high steam pressure and water evaporation from the dentin structure; these lead to the oxidation of organic components, melting and fast recrystallization of apatite crystals [37, 38]. However, Er:YAG laser promote micro-cracks and changes in the chemical composition of the organic

Table 2 Average (standard deviation) of microhardness values (KHN) found for the interaction of depth vs treatment

Treatment	Depth		
	30 μm	60 μm	90 μm
Untreated	18.78 (5.02) ^{A,a}	25.65 (11.43) ^{B,a}	29.60 (13.85) ^{C,a}
Nchi	25.40 (8.75) ^{A,a,b}	25.75 (8.86) ^{A,a}	26.73 (8.53) ^{A,a}
Gt+Nchi	26.17 (10.62) ^{A,b}	26.02 (11.64) ^{A,a}	28.17 (13.75) ^{A,a}

Different capital letters indicate a statistically significant difference in the same line

Different lowercase letters indicate a statistically significant difference in the same column

Three-way ANOVA, Tukey's post hoc test ($\alpha=0.05$)

dentin matrix [37, 39] which could compromise the durability of adhesive restorations.

For this reason, the nanoformulation based on green tea-loaded chitosan nanoparticles (Gt+Nchi) was applied after caries excavation on leathery dentin and the subsurface microhardness was evaluated. At 30 μm from the surface, the Gt+Nchi biomodification increased the subsurface microhardness of dentin when compared to untreated group. When dentin was biomodified with Nchi and Gt+Nchi, there was no difference between depths evaluated, showing both nanoformulations may modify the mechanical properties of dentin, which could be due the reduction of dentin porosities. Dentin contains about between 18,000 and 21,000/ mm^2 dentinal tubules, with more numerous tubules in the inner third layer than the outer third layer of the dentin. The diameter of tubules varies between 2 and 4 μm [40]. The nanoparticles reached an average size of less than 350 nm which allowed its penetration through the tubules, increasing the directly interaction with collagen fibrils. The $-\text{COOH}$ and NH_2 groups present in collagen may form hydrogen bonds with $-\text{OH}$ and $-\text{NH}_2$ groups from chitosan, especially because chitosan contains large numbers of $-\text{OH}$ groups. The long chain of chitosan may wind around the collagen triple helix and the interaction of these two different molecules may form a complex [41]. In addition, chitosan as a cationic polysaccharide may be bonded ionically to the anionic $-\text{COOH}$ group present in collagen [41, 42]. Furthermore, the catechol moieties present in the green tea extract interact with collagen inducing stable cross-linking interactions between the hydroxyl and carbonyl groups of the collagen—via the hydroxyl, carboxyl, amine-or amine functional groups [43–45]. In addition, green tea increased microhardness of dentin by the formation of deposits of organic materials on its surface. This can be attributed to the presence of green tea-induced collagen cross-linking [29].

Green tea extract activity may be reduced by factors such as temperature, pH, light, oxygen and enzyme activity [46]. After the drying process, green tea extract has highly

hygroscopic potential and is sticky due the presence of sugars. Thus, the water absorption can easily degrade the catechins [30, 31]. For those reasons, chitosan nanoparticles may be an appropriate approach to protect the green tea extract from chemical and/or enzymatic degradation [22]. As expected, this is the same effect of many different nanoparticles that have been used as to encapsulant or shell to protect bioactive compounds. They are loaded inside the “core” protecting from direct contact with light, heat and oxygen, the most common degradation agents [47]. Chitosan enables a degree of chemical modification at amino ($-\text{NH}_2$) and hydroxyl ($-\text{OH}$) groups [48]. In the present study, nanoformulations were prepared by means of ionic gelation technique which is organic solvent free, non-toxic, convenient and controllable process [49]. This method is based on the ionic interactions between the positively charged primary amino groups of chitosan, and the negatively charged groups of sodium tripolyphosphate (TPP). TPP is a polyanion highly used as ion cross-linking agent due to its non-toxic and multivalent properties [50].

Nanoparticles were synthesized from a low molecular weight chitosan, between 20 and 190 kDa with degree of deacetylation 75–85%, since it shows better solubility, biocompatibility, bioactivity, and biodegradability when compared to the high molecular weight chitosan [27]. Chitosan is soluble in acidic medium, at pH below 6.0, due to the quaternization of the amine groups with pKa value of 6.3, making chitosan a water-soluble cationic polyelectrolyte. At low pH, amines group get protonated and become positively charged, making chitosan a water-soluble cationic polyelectrolyte [46]. There are also, hydrogen bonding interactions between chitosan molecules. A concentration of chitosan below 2.0 mg/mL allows an equilibrium between the hydrogen bonding attraction and the intermolecular electrostatic repulsion [49]. Differently, at pH above 6, amine groups present in chitosan become deprotonated, chitosan loses its charge, becoming insoluble. Thus, the pKa value between 6 and 6.5 determine the solubility or insolubility of chitosan [51]. In the present study, the zeta potential of chitosan nanoparticles is around +30 mV, considered strongly cationic. The presence of amino groups in the polymeric chain prevents the aggregation of the nanoparticles. Some studies assimilate the zeta potential to one of the factors that help the particles not to aggregate and, therefore, refer to stability. The density of the surface charge, in this case around 30 Mv, refers to the charges present that will repel each other [52].

Limited data about the mechanical properties of remaining dentin are available [53]. Microhardness testing has been used in vitro studies to determine the changes in the consistency of the dental hard tissues after being subjected to different types of treatments [54]. However, other mechanical properties should be assessed to obtain a complete understanding about the dentin response to the treatment

proposed. In addition, inherent limitations about microhardness testing as the problems of accuracy, repeatability, and correlation must be pointed out. However, using properly maintained and calibrated equipment, trained personnel, and appropriate testing environments, testing error and variability can be minimized. Nanomaterials based on chitosan associated with other natural compounds, as the green tea extract, may be a potential strategy to restore or reinforce the dentin organic matrix. Chemical composition and bond stability of the remaining dentin treated with chitosan-based nanoparticles containing green tea should be assessed in future studies.

Conclusions

- Both nanoformulations showed an average size less than 350 nm with nanoparticles of different sizes and stability along the 90-day period evaluated.
- The subsurface microhardness of bur-treated and laser-irradiated dentin was similar.
- At 30 μm , the biomodification with Gt + Nchi improved the microhardness of leathery dentin, independently of caries excavation method used.

Acknowledgements F.A.C.Z, G.T.C.L and S.A.M.C would like to thank the São Paulo Research Foundation (FAPESP) for the scholarships [#2017/11582-1, #2019/04807-2] awarded, and the Brazilian Federal Agency for Support and Evaluation of Graduate Education—CAPES, Brazil. A.C.T and L.A.U.T also thank FAPESP [Thematic project #2013/50181-1] for the financial support. Authors would like Ana Paula Macedo for assistance with statistical data analysis and Viviane de Cássia Oliveira for support with microbiological experiments.

Declarations

Conflict of interest The authors declare that they have no conflict of interest.

References

1. Banerjee A, Frencken JE, Schwendicke F, Innes NPT. Contemporary operative caries management: consensus recommendations on minimally invasive caries removal. *Br Dent J.* 2017;223:215–22. <https://doi.org/10.1038/sj.bdj.2017.672> (Nature Publishing Group).
2. Ricketts D, Innes N, Schwendicke F. Selective removal of carious tissue. *Monogr Oral Sci.* 2018;27:82–91.
3. MacEdo GV, Yamauchi M, Bedran-Russo AK. Effects of chemical cross-linkers on caries-affected dentin bonding. *J Dent Res.* 2009;88:1096–100.
4. Liu Y, Yao Y, Liu YW, Wang Y. A Fourier transform infrared spectroscopy analysis of carious dentin from transparent zone to normal zone. *Caries Res.* 2014;48:320–9.
5. Curylofo-Zotti FA, Tanta GS, Zucoloto ML, Souza-Gabriel AE, Corona SAM. Selective removal of carious lesion with Er:YAG laser followed by dentin biomodification with chitosan. *Lasers Med Sci.* 2017;32:1595–603.
6. Curylofo-Zotti FA, Scheffel DLS, Macedo AP, Souza-Gabriel AE, Hebling J, Corona SAM. Effect of Er:YAG laser irradiation and chitosan biomodification on the stability of resin/demineralized bovine dentin bond. *J Mech Behav Biomed Mater.* 2019;91:220–8.
7. Li T, Zhang X, Shi H, Ma Z, Lv B, Xie M. Er:YAG laser application in caries removal and cavity preparation in children: a meta-analysis. *Lasers Med Sci.* 2019;34:273–80.
8. Polizeli SAF, Curylofo-Zotti FA, Valério RA, Nemezio MA, Souza-Gabriel AE, Borsatto MC, et al. Selective removal of necrotic dentin in primary teeth using laser irradiation: One-year clinical evaluation of composite restorations. *J Lasers Med Sci.* 2019;10:108–16.
9. Valério RA, Galo R, Galafassi D, Corona SAM, Borsatto MC. Four-year clinical prospective follow-up of resin composite restoration after selective caries removal using Er:YAG laser. *Clin Oral Investig.* 2020;24(7):2271–83.
10. Hibst R, Keller U. Experimental studies of the application of the Er:YAG laser on dental hard substances: I. Measurement of the ablation rate. *Lasers Surg Med.* 1989;9:338–44.
11. Fornaini C. Er:YAG and adhesion in conservative dentistry: clinical overview. *Laser Ther.* 2013;22:31–5.
12. Dommisch H, Peus K, Kneist S, Krause F, Braun A, Hedderich J, et al. Fluorescence-controlled Er:YAG laser for caries removal in permanent teeth: a randomized clinical trial. *Eur J Oral Sci.* 2008;116:170–6.
13. Merigo E, Fornaini C, Clini F, Fontana M, Cella L, Oppici A. Er:YAG laser dentistry in special needs patients. *Laser Ther.* 2015;24:189–93.
14. Ito S, Saito T, Tay FR, Carvalho RM, Yoshiyama M, Pashley DH. Water content and apparent stiffness of non-caries versus caries-affected human dentin. *J Biomed Mater Res B Appl Biomater.* 2005;72:109–16.
15. Keller U, Hibst R. Effects of Er:YAG laser in caries treatment: a clinical pilot study. *Lasers Surg Med.* 1997;20:32–8.
16. Rizeq BR, Younes NN, Rasool K, Nasrallah GK. Synthesis, bioapplications, and toxicity evaluation of chitosan-based nanoparticles. *Int J Mol Sci.* 2019;20:5776.
17. Domard A. A perspective on 30 years research on chitin and chitosan. *Carbohydr Polym.* 2011;84:696–703.
18. Muxika A, Etxabide A, Uranga J, Guerrero P, de la Caba K. Chitosan as a bioactive polymer: Processing, properties and applications. *Int J Biol Macromol.* 2017;105:1358–68. <https://doi.org/10.1016/j.ijbiomac.2017.07.087> (Elsevier B.V.).
19. Cavalcante LLR, Tedesco AC, Takahashi LAU, Curylofo-Zotti FA, Souza-Gabriel AE, Corona SAM. Conjugate of chitosan nanoparticles with chloroaluminium phthalocyanine: Synthesis, characterization and photoinactivation of *Streptococcus mutans* biofilm. *Photodiagnosis Photodyn Ther.* 2020;30:101709. <https://doi.org/10.1016/j.pdpdt.2020.101709> (Elsevier).
20. Gu LS, Cai X, Guo JM, Pashley DH, Breschi L, Xu HHK, et al. Chitosan-based extrafibrillar demineralization for dentin bonding. *J Dent Res.* 2019;98:186–93. <https://doi.org/10.1177/0022034518805419>.
21. Kawakita ERH, Ré ACS, Peixoto MPG, Ferreira MP, Ricomini-Filho AP, Freitas O, et al. Effect of chitosan dispersion and micro-particles on older streptococcus mutans biofilms. *Molecules.* 2019;24:1–11.
22. Cánepa C, Imperiale JC, Berini CA, Lewicki M, Sosnik A, Bigli-one MM. Development of a drug delivery system based on chitosan nanoparticles for oral administration of interferon- α . *Biomacromol.* 2017;18:3302–9.
23. Matshetshe KI, Parani S, Manki SM, Oluwafemi OS. Preparation, characterization and in vitro release study of β -cyclodextrin/

- chitosan nanoparticles loaded Cinnamomum zeylanicum essential oil. *Int J Biol Macromol*. 2018;118:676–82. <https://doi.org/10.1016/j.ijbiomac.2018.06.125> (Elsevier B.V).
24. Rahimi S, Khoe S, Ghandi M. Development of photo and pH dual crosslinked coumarin-containing chitosan nanoparticles for controlled drug release. *Carbohydr Polym*. 2018;201:236–45. <https://doi.org/10.1016/j.carbpol.2018.08.074> (Elsevier Ltd).
 25. Reygaert WC. Green tea catechins: their use in treating and preventing infectious diseases. *Biomed Res Int*. 2018;2018:1–9 (Hindawi).
 26. Smeriglio A, Barreca D, Bellocco E, Trombetta D. Proanthocyanidins and hydrolysable tannins: occurrence, dietary intake and pharmacological effects. *Br J Pharmacol*. 2017;174:1244–62.
 27. Younes I, Rinaudo M. Chitin and chitosan preparation from marine sources. Structure, properties and applications. *Mar Drugs*. 2015;13:1133–74.
 28. Arnaud TMS, De Barros NB, Diniz FB. Chitosan effect on dental enamel de-remineralization: an in vitro evaluation. *J Dent*. 2010;38:848–52.
 29. Mirkarimi M, Toomarian L. Effect of green tea extract on the treatment of dentin erosion: an in vitro study. *J Dent (Tehran)*. 2012;9:224–8.
 30. Cai ZY, Li XM, Liang JP, Xiang LP, Wang KR, Shi YL, et al. Bioavailability of tea catechins and its improvement. *Molecules*. 2018;23:10–3.
 31. Zeng L, Ma M, Li C, Luo L. Stability of tea polyphenols solution with different pH at different temperatures. *Int J Food Prop*. 2017;20:1–18. <https://doi.org/10.1080/10942912.2014.983605> (Taylor & Francis).
 32. Marquezan M, Corrêa FNP, Sanabe ME, Rodrigues Filho LE, Hebling J, Guedes-Pinto AC, et al. Artificial methods of dentine caries induction: a hardness and morphological comparative study. *Arch Oral Biol*. 2009;54:1111–7.
 33. Rasheed M. Hardness Testing. *Chart Mech Eng*. 1978;25(9):79–80.
 34. Abou Neel EA, Anas A, Strange A, Salwa I, Coathup M, Young AM, et al. Demineralization-remineralization dynamics in teeth and bone. *Int J Nanomedicine*. 2016;11:4735–63.
 35. Featherstone JDB. The continuum of dental caries—evidence for a dynamic disease process. *J Dent Res*. 2004;83:2002–5.
 36. Baraba A, Perhavec T, Chieffi N, Ferrari M, Anić I, Miletić I. Ablative potential of four different pulses of Er:YAG lasers and low-speed hand piece. *Photomed Laser Surg*. 2012;30:301–7.
 37. He Z, Chen L, Hu X, Shimada Y, Otsuki M, Tagami J, et al. Mechanical properties and molecular structure analysis of sub-surface dentin after Er:YAG laser irradiation. *J Mech Behav Biomed Mater [Internet]*. 2017;74:274–82. <https://doi.org/10.1016/j.jmbbm.2017.05.036> (Elsevier Ltd).
 38. Vogel A, Venugopalan V. Mechanisms of pulsed laser ablation of biological tissues. *Chem Rev*. 2003;103:577–644.
 39. Cardoso MV, De Almeida NA, Mine A, Coutinho E, Van Landuyt K, De Munck J, et al. Current aspects on bonding effectiveness and stability in adhesive dentistry. *Aust Dent J*. 2011;56:31–44.
 40. Lenzi TL, Guglielmi CDAB, Arana-chavez VE, Raggio DP. Microscopy microanalysis tubule density and diameter in coronal dentin from primary and permanent human teeth. *Microsc Microanal*. 2013;19(6):1445–9.
 41. Sionkowska A, Wisniewski M, Skopinska J, Kennedy CJ, Wess TJ. Molecular interactions in collagen and chitosan blends. *Biomaterials*. 2004;25:795–801.
 42. Kishen A, Shrestha S, Shrestha A, Cheng C, Goh C. Characterizing the collagen stabilizing effect of crosslinked chitosan nanoparticles against collagenase degradation. *Dent Mater*. 2016;32:968–77.
 43. Aguiar TR, Vidal CMP, Phansalkar RS, Todorova I, Napolitano JG, McAlpine JB, et al. Dentin biomodification potential depends on polyphenol source. *J Dent Res*. 2014;93:417–22.
 44. Han B, Jaurequi J, Tang BW, Nimmi ME. Proanthocyanidin: a natural crosslinking reagent for stabilizing collagen matrices. *J Biomed Mater Res A*. 2003;65:118–24.
 45. He L, Mu C, Shi J, Zhang Q, Shi B, Lin W. Modification of collagen with a natural cross-linker, procyanidin. *Int J Biol Macromol*. 2011;48:354–9. <https://doi.org/10.1016/j.ijbiomac.2010.12.012> (Elsevier B.V.).
 46. Zokti JA, Baharin BS, Mohammed AS, Abas F. Green tea leaves extract: Microencapsulation, physicochemical and storage stability study. *Molecules*. 2016;21:1–24.
 47. Keawchaon L, Yoksan R. Preparation, characterization and in vitro release study of carvacrol-loaded chitosan nanoparticles. *Colloids Surfaces B Biointerfaces*. 2011;84:163–71. <https://doi.org/10.1016/j.colsurfb.2010.12.031>.
 48. Kunjachan S, Jose S. Understanding the mechanism of ionic gelation for synthesis of chitosan nanoparticles using qualitative techniques. *Asian J Pharm*. 2010;4:148–53.
 49. Fan W, Yan W, Xu Z, Ni H. Formation mechanism of monodisperse, low molecular weight chitosan nanoparticles by ionic gelation technique. *Colloids Surfaces B Biointerfaces*. 2012;90:21–7. <https://doi.org/10.1016/j.colsurfb.2011.09.042> (Elsevier B.V.).
 50. Shu XZ, Zhu KJ. The influence of multivalent phosphate structure on the properties of ionically cross-linked chitosan films for controlled drug release. *Eur J Pharm Biopharm*. 2002;54:235–43.
 51. Roy JC, Salaün F, Giraud S, Ferri A, Chen G, Guan J. Solubility of chitin: solvents, solution behaviors and their related mechanisms. In: *Solubility of polysaccharides 2017*. <https://doi.org/10.5772/intechopen.71385>
 52. Siqueira-Moura MP, Primo FL, Espreafico EM, Tedesco AC. Development, characterization, and photocytotoxicity assessment on human melanoma of chloroaluminum phthalocyanine nanocapsules. *Mater Sci Eng C*. 2013;33:1744–52.
 53. Joves GJ, Inoue G, Sadr A, Nikaido T, Tagami J. Nanoindentation hardness of intertubular dentin in sound, demineralized and natural caries-affected dentin. *J Mech Behav Biomed Mater*. 2014;32:39–45.
 54. Kirsten GA, Takahashi MK, Rached RN, Giannini M, Souza EM. Microhardness of dentin underneath fluoride-releasing adhesive systems subjected to cariogenic challenge and fluoride therapy. *J Dent*. 2010;38:460–8. <https://doi.org/10.1016/j.jdent.2010.02.006> (Elsevier Ltd).

Publisher's Note Springer Nature remains neutral with regard to jurisdictional claims in published maps and institutional affiliations.